frontiers in Marine Science

ORIGINAL RESEARCH
published: 24 March 2021
doi: 10.3389/fmars.2021.622319

The Combined Effects of Increased pCO_2 and Warming on a Coastal Phytoplankton Assemblage: From Species Composition to Sinking Rate

Yuanyuan Feng[1], Fei Chai[2,3], Mark L. Wells[2,3], Yan Liao[1], Pengfei Li[1], Ting Cai[1], Ting Zhao[1], Feixue Fu[4] and David A. Hutchins[4]*

[1] College of Marine and Environmental Sciences, Tianjin University of Science and Technology, Tianjin, China, [2] State Key Laboratory of Satellite Ocean Environment Dynamics, Second Institute of Oceanography, Ministry of Natural Resources, Hangzhou, China, [3] School of Marine Sciences, University of Maine, Orono, ME, United States, [4] Department of Biological Sciences, University of Southern California, Los Angeles, CA, United States

OPEN ACCESS

Edited by:
Xianghui Guo, Xiamen University, China

Reviewed by:
Allanah J. Paul, GEOMAR Helmholtz Centre for Ocean Research Kiel, Germany
Gang Li, South China Sea Institute of Oceanology (CAS), China
Kalle Olli, Estonian University of Life Sciences, Estonia

***Correspondence:**
Yuanyuan Feng
yfeng@tust.edu.cn;
yyfengcocco@126.com

Specialty section:
This article was submitted to Coastal Ocean Processes, a section of the journal Frontiers in Marine Science

Received: *28 October 2020*
Accepted: *03 March 2021*
Published: *24 March 2021*

Citation:
Feng Y, Chai F, Wells ML, Liao Y, Li P, Cai T, Zhao T, Fu F and Hutchins DA (2021) The Combined Effects of Increased pCO_2 and Warming on a Coastal Phytoplankton Assemblage: From Species Composition to Sinking Rate. Front. Mar. Sci. 8:622319. doi: 10.3389/fmars.2021.622319

In addition to ocean acidification, a significant recent warming trend in Chinese coastal waters has received much attention. However, studies of the combined effects of warming and acidification on natural coastal phytoplankton assemblages here are scarce. We conducted a continuous incubation experiment with a natural spring phytoplankton assemblage collected from the Bohai Sea near Tianjin. Experimental treatments used a full factorial combination of temperature (7 and 11°C) and pCO_2 (400 and 800 ppm) treatments. Results suggest that changes in pCO_2 and temperature had both individual and interactive effects on phytoplankton species composition and elemental stoichiometry. Warming mainly favored the accumulation of picoplankton and dinoflagellate biomass. Increased pCO_2 significantly increased particulate organic carbon to particulate organic phosphorus (C:P) and particulate organic carbon to biogenic silica (C:BSi) ratios, and decreased total diatom abundance; in the meanwhile, higher pCO_2 significantly increased the ratio of centric to pennate diatom abundance. Warming and increased pCO_2 both greatly decreased the proportion of diatoms to dinoflagellates. The highest chlorophyll *a* biomass was observed in the high pCO_2, high temperature phytoplankton assemblage, which also had the slowest sinking rate of all treatments. Overall, there were significant interactive effects of increased pCO_2 and warming on dinoflagellate abundance, pennate diatom abundance, diatom vs. dinoflagellates ratio and the centric vs. pennate ratio. These findings suggest that future ocean acidification and warming trends may individually and cumulatively affect coastal biogeochemistry and carbon fluxes through shifts in phytoplankton species composition and sinking rates.

Keywords: ocean acidification, warming, phytoplankton, diatoms, biogenic silica, sinking rate, coastal environment

INTRODUCTION

Anthropogenic activities have increased atmospheric pCO_2 at a rate of ∼1.8 ppm per year over the last century (IPCC, 2014), with surface seawaters absorbing ∼25% of these CO_2 emissions (Le Quéré et al., 2016). This results in increased CO_2 and HCO_3^- concentrations and decreased pH and CO_3^{2-} concentrations in surface seawaters, collectively referred to as "ocean acidification (OA)" (Caldeira and Wickett, 2003). The average pH of ocean surface waters is predicted to fall from ∼8.1 to ∼7.8 by the end of this century (Feely et al., 2009). In addition, coastal seawater carbonate chemistry can be affected by organic- and acidic sulfate-rich freshwater runoff (Fitzer et al., 2018), or the respiration of organic matter produced as a consequence of eutrophication (Cai et al., 2011), and thus coastal ecosystems are expected to experience more severe acidification (Zhai et al., 2012).

In addition to OA, increasing atmospheric CO_2 also has elevated sea surface temperatures (SST) as a consequence of the greenhouse effect, with predicted 1 to 4°C increases in SST over the next 100 years (Bopp et al., 2013). Observed warming trends are not homogeneous between coastal and oceanic regions (Varela et al., 2018). For example, in Chinese coastal waters, a significant warming trend of ∼0.8–2°C per century has been observed in recent years, almost double that of global SST (Carton and Giese, 2008; Feng and Lin, 2009; Wu et al., 2017).

Both CO_2 and temperature are important environmental drivers controlling marine phytoplankton physiology. The low CO_2 concentrations in seawater can limit the photosynthetic activities of some groups of marine phytoplankton due to the low affinity of the enzyme Ribulose-1,5-bisphosphate carboxylase/oxygenase (RubisCO) for dissolved CO_2 (Riebesell et al., 1993; Falkowski and Raven, 2007). As a consequence, phytoplankton have evolved carbon concentrating mechanisms (CCMs) to enhance carbon availability, but the efficiencies of CCMs differ among groups and taxa. Consequently, the increases in CO_2 concentrations with ocean acidification may have disproportionate effects among different phytoplankton groups/species. For instance, CO_2 enrichment promoted the photosynthetic efficiency of the marine coccolithophore *Emiliania huxleyi* more than the diatom *Skeletonema costatum* or the flagellate *Phaeocystis globosa* (Rost et al., 2003). Rising pCO_2 could thus lead to shifts in phytoplankton taxonomic composition and species succession in the natural environment (Schulz et al., 2017; Bach and Taucher, 2019). It has been shown that CO_2 enrichment can cause a shift in dominance from small pennate to larger centric diatom species in a Southern Ocean phytoplankton community (Tortell et al., 2008; Feng et al., 2010), whereas some other studies found little effect of changing CO_2 concentration on the composition of a coastal phytoplankton assemblage (Kim et al., 2006). In addition, changes in pCO_2 may also play an important role in regulating the biomineralization of calcifying coccolithophores (Raven and Crawfurd, 2012) and siliceous diatoms (Milligan et al., 2004), as well as other physiological processes that alter the overall elemental stoichiometry of phytoplankton (Burkhardt et al., 1999; Hutchins et al., 2009; Finkel et al., 2010). During the past decades, numerous studies have especially focused on the sensitivity of calcification process to ocean acidification, with a general trend of weakened calcification (Riebesell et al., 2000; Beaufort et al., 2011; Krumhardt et al., 2017). While for the silicification process of diatoms, although theoretically the formation of biogenic silica should be facilitated at lower pH (Martin-Jézéquel et al., 2000), controversial results has been reported (Milligan et al., 2004). All of these changes will in turn profoundly influence marine biogeochemical cycles.

Temperature is one of the most fundamental environmental drivers determining the growth, metabolic activities, elemental composition, and distribution of marine phytoplankton (Eppley, 1972). Warming has induced changes in geographic distribution, harmful algal bloom intensity, and biodiversity in marine ecosystems (reviewed by Sommer et al., 2012; Hutchins and Fu, 2017). Previous studies have suggested that CO_2 enrichment and warming may have combined or interactive effects on phytoplankton physiology (Hutchins et al., 2007; Feng et al., 2008) and species succession and biogeochemistry of natural phytoplankton communities (Hare et al., 2007b; Feng et al., 2009; Sommer et al., 2015; Sett et al., 2018).

However, studies examining the influence of multiple environmental driver interactions on marine life are scarce, and more understanding is needed, especially at the community level (Joint et al., 2011; Boyd et al., 2018). Here we present a continuous incubation experiment that investigated the interactive effects of increased pCO_2 and warming on a natural marine phytoplankton assemblage collected from coastal Bohai Sea waters near Tianjin, China, in a region impacted by intense anthropogenic activity. The objective of this study was to investigate the effects of future environmental changes of increased CO_2 concentration and temperature both individually and interactively on phytoplankton assemblage succession, elemental composition, and community sinking rates. The findings help us to understand the consequences of future increases in environmental stressors for biogeochemical processes such as carbon export and elemental cycling by coastal phytoplankton assemblages.

MATERIALS AND METHODS

Experimental Setup and Sampling

Seawater just below the surface (<5 m depth) containing the intact coastal phytoplankton assemblage was collected using a Niskin sampler deployed from a pier near the Tianjin Coastal Recreational Area, Bohai Bay (39.10°N, 117.84°E; temperature: 7°C; salinity: 31; pH: 8.02; nitrate: 8.1 μM; phosphate: 0.4 μM; silicate: 4.2 μM) on March 15, 2017. The whole water was filtered through 100 μm Nitex mesh to eliminate large zooplankton, and then dispensed into 12 4-L clear polycarbonate bottles for incubation. The measured Chl-*a* biomass was low on the 100 μm Nitex mesh, having little effects on the remaining phytoplankton assemblages. Seawater (∼500 L) collected at the same sampling site was filtered through 0.2 μm in-line filters and stored in 25 L clean carboys, to be used for making dilution medium during the continuous culture incubation experiment.

A continuous culture incubation system (Hutchins et al., 2003; Hare et al., 2005, 2007a,b; Feng et al., 2009, 2010) was used to carry out an outdoor experiment under model projected pCO_2 and temperature conditions for the end of this century under some scenarios (IPCC, 2014). Four experimental treatments from full factorial combination of temperature (7 and 11°C) and pCO_2 (400 and 800 ppm) were examined in triplicate bottles: (1) control: 7°C and 400 ppm pCO_2; (2) high pCO_2: 7°C and 800 ppm pCO_2; (3) high temperature: 11°C and 400 ppm pCO_2; and (4) combined: 11°C and 800 ppm pCO_2. Nutrient stock solutions were added to both the initial incubation bottles and the filtered seawater medium to final concentrations of 10 μM nitrate, 1 μM phosphate, and 10 μM silicate. Light levels for the incubations were adjusted using neutral density screens to provide an irradiance of 50% of the incident sea surface level (I_0). The incubation temperatures were maintained by submersing the bottles in a circulating water bath connected to temperature control systems (HC1000BC, Hailea, China) via water pumps. Two different CO_2 levels were adjusted in both the incubation bottles and carboys containing the filtered seawater for dilution, by gentle bubbling (∼4 mL min^{-1}) of ambient air (∼400 ppm) and an air/CO_2 mixture with pCO_2 level of 800 ppm controlled by a gas mixer (CE100, Ruihua, China). The bubbling of the incubation bottles and seawater medium was continuous throughout the whole incubation period in order to maintain the seawater carbonate chemistry.

The phytoplankton community was grown in batch mode during the first 3 days of incubation. The continuous incubation mode with a dilution rate of 0.4 d^{-1} was started on the fourth day (T3) by turning on the peristaltic pumps (Shenchen, China) connected to the bottles through inflow lines going into the bottles from the caps. The dilution rate was chosen based on the average growth rate of the early spring phytoplankton assemblages under nutrient replete conditions in the Bohai Sea (Zou et al., 2001). The outflow outlets were connected at the shoulders of the bottles, in order to maintain a constant volume in the bottles. The bottles were gently shaken and mixed 5–7 times a day to ensure the phytoplankton cells remained suspended.

Samples for pH and total chlorophyll *a* (Chl-*a*) measurements were taken daily directly from the incubation bottles. The daily sampling volume was limited to less than 10% of the incubation volume to avoid significant perturbations of the biomass equilibrium (Feng et al., 2009). Size-fractionated Chl-*a* was sampled only on T0, T3, and T21. The continuous incubation was ended on T21, and samples for measurements of dissolved inorganic carbon (DIC), pH, total alkalinity, Chl-*a*, phytoplankton community structure, biogenic silica (BSi), particulate organic carbon (POC), particulate organic nitrogen (PON), particulate organic phosphorus (POP) and sinking rates were taken on T0 and the final sampling day. T0 samples were taken from the 100 μm Nitex mesh filtered source seawater in triplicates.

Sample Analysis

Seawater Carbonate Chemistry Measurements

Two hundred and fifty mL samples for total alkalinity analysis were preserved with 200 μL of 5% $HgCl_2$ solution in Shott glass bottles (Shott AG, Germany) with screw caps. Alkalinity was then measured using potentiometric titration following the method of Dickson et al. (2007). The accuracy of the method as determined by analysis of Certified Reference Material provided by Andrew Dickson from Scripps Institution of Oceanography was estimated to be ±2 μmol kg^{-1}. Samples for DIC measurements were fixed in 20 mL borosilicate vials with addition of 0.2 mL of 5% $HgCl_2$ solution. The DIC concentration was measured using a total inorganic carbon analyzer (CM140, UIC, United States) by acidification and coulometric detection, and corrected to the Dickson seawater standards (Dickson et al., 2007). The estimated accuracy of the analysis was ± 5 μmol kg^{-1}. pH values were checked daily using a pH meter (S210-B, Mettler Toledo) calibrated with commercial NBS buffers. The seawater carbonate chemistry (data shown in **Supplementary Table 1**, output at the incubation temperatures) was calculated using the program CO2sys (E. Lewis and D. W. R. Wallace) with measured DIC and alkalinity values, using the constants in Mehrbach et al. (1973), re-fitted by Dickson and Millero (1987).

Phytoplankton Chl-*a* Biomass and Assemblage Structure Analyses

20–30 mL samples for Chl-*a* analysis were filtered and extracted in 90% acetone at –20°C in the dark for 24 h, and then measured using a Turner Trilogy fluorometer. Samples for total Chl-*a* biomass analysis were filtered through 0.2 μm polycarbonate filters (Millipore, United States); while size-fractionated Chl-*a* was filtered onto 0.2, 2, and 20 μm polycarbonate filters (Millipore, United States) in series. Samples for phytoplankton taxonomic analysis were preserved with a final concentration of 1% glutaraldehyde and stored at 4°C until analysis. The samples were then concentrated using a 25 mL Utermöhl cell count chamber and counted at 400× magnification under an inverted microscope (AE2000, Motic, China) (Utermöhl, 1958; Thomas, 1997).

Particulate Matter

POC and PON samples (30 mL) were filtered onto pre-combusted (450°C, 2 h) GF/F glass fiber filters (Whatman, United States) and then dried at 55°C. C and N elemental composition was then measured with an elemental analyzer (270, Costech Analytical Technologies, Italy). Thirty mL samples for BSi analysis were filtered onto 0.6 μm polycarbonate filters (Millipore, United States), dried at 60°C, and analyzed using the spectrophotometric method following Brzezinski and Nelson (1995). POP samples (30 mL) were filtered onto pre-combusted GF/F glass fiber filters (Whatman, United States), rinsed with 2 mL of 0.17 mol L^{-1} Na_2SO_4, stored in pre-combusted borosilicate vials with addition of 2 mL of 0.017 mol L^{-1} $MgSO_4$. The samples were then dried and analyzed following the molybdate colorimetric method (Solórzano and Sharp, 1980).

Phytoplankton Sinking Rate

The sinking rate of the phytoplankton assemblage based on Chl-*a* measurements was determined in triplicate samples using the SETCOL method as described in Bienfang (1981). In brief, a plexiglass column (4 cm in diameter, 1 m in length) was filled

up to the top with a homogeneous seawater sample containing the whole phytoplankton assemblage and covered tightly with a glass lid. The column was placed in the dark at the corresponding incubation temperature for a settling time of 3 h, yielding a maximum measurable sinking rate of 8 m d^{-1}. The settling was terminated by carefully draining the upper, middle, and bottom compartments of the column through valved tubing connected through the wall of the column at each depth. The total Chl-*a* concentration of each compartment was then measured, and the sinking rate was calculated using the following equation:

$$S = (C_b \times V_b)/(C_u \times V_u + C_m \times V_m + C_b \times V_b) \times L/t. \quad (1)$$

Here, S is the sinking rate; C_u, C_m, and C_b are the Chl-*a* concentrations in the upper, middle and bottom compartments of the sinking column, respectively; V_u, V_m, and V_b are the volumes in the upper, middle, and bottom compartments, respectively; L is the length of the column; and t is the total sinking time (Bienfang, 1981).

Data Analysis

Statistics

A two-way ANOVA test was used to detect two-way interactions among temperature and CO_2 with the assumptions of homogeneity of variance, independence of observations and independent distribution of variables. Pair-wise tests were conducted using Tukey's multiple comparison *post hoc* analysis. The statistical analysis was performed using GraphPadPrism 7.0 software (GraphPad Software, Inc., San Diego, CA, United States).

Types of Driver Interactions

Two-way interactions among temperature and CO_2 were determined by quantitative comparisons between the observed effects and the model predicted effects of two drivers. The observed effect was calculated as the percentage of change between the combined treatment and control treatment. A model was used for the predictions of two-way effects (Folt et al., 1999; Liao et al., 2019; Feng et al., 2020):

$$\text{Multiplicative effect} = (1 + E_1) \times (1 + E_2) - 1. \quad (2)$$

Here, E1 and E2 denote the individual observed effect of increased pCO_2 and warming on the measured parameter, respectively, calculated as the percentage of changes relative to control treatment.

The interactions among increased pCO_2 and warming were defined as follows:

(1) Synergistic interactive effect: the observed effect > the calculated multiplicative effect (Folt et al., 1999; Boyd and Hutchins, 2012; Boyd et al., 2018);
(2) Antagonistic interactive effect: the observed effect < the calculated multiplicative effect (Folt et al., 1999; Boyd and Hutchins, 2012; Boyd et al., 2018).

Both synergistic and antagonistic interactive effects can be positive (increase) or negative (decrease).

RESULTS

Total and Size-Fractionated Chl-*a* Biomass

The total phytoplankton Chl-*a* biomass kept increasing quickly in the four experimental treatments in the first 5 days of the incubation period (**Figure 1**). The total Chl-*a* concentration on T0 at the sampling site was 14.4 ± 1.4 μg L^{-1}, and it increased throughout the 3-day batch incubation mode. The average value of the total Chl-*a* concentration in the control treatment was lower than those in the other three treatments during the entire course of the incubation (**Figure 1**). By T5, the Chl-*a* concentration in all four treatments were more than double the T0 value, with the highest value observed in the combined

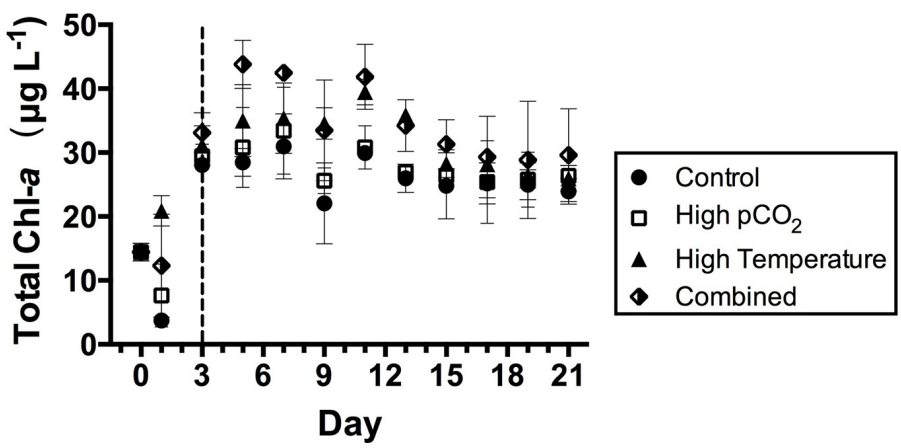

FIGURE 1 | Total Chl-*a* concentrations during the time course of the incubation in the four experimental treatments. Values are the means and error bars are the standard deviations of triplicates. The dashed line separates the two incubation stages: T0–T3 batch growth mode, and T3–T21 continuous growth code with dilution rate of 0.4 d^{-1}.

treatment. During the first 5 days of incubation, the total Chl-*a* concentration was overall higher the two higher temperature treatments (high temperature and combined) compared to that under control and high pCO_2 (**Figure 1**). The total Chl-*a* biomass declined in all the experimental treatments from T11 to T15 and the differences between treatments became less than those in the earlier stage of the incubation. The values also became relatively stable as growth and dilution rates came into balance starting from T15 until the final sampling day (T21, **Figure 1**).

Phytoplankton Chl-*a* biomass size-fractions responded differently to changes in temperature and pCO_2 conditions (**Figure 2**). The initial (T0) phytoplankton assemblage collected for the incubation was dominated by nano-phytoplankton (2–20 μm), contributing 74.5% of the total Chl-*a* biomass. The micro-phytoplankton (>20 μm) and pico-phytoplankton accounted for 18.0 and 7.50% of the total Chl-*a* biomass, respectively (**Figure 2**). The nano-phytoplankton continued to dominate the Chl-*a* biomass (>60%) during the incubation in all the experimental treatments. On the final sampling day, there was a general trend of relatively lower percentages of micro-phytoplankton Chl-*a* biomass but higher percentage of nano-phytoplankton and pico-phytoplankton Chl-*a* biomass under higher temperature. The percentage of Chl-*a* biomass in the micro-phytoplankton group was in general lower in the elevated temperature (high temperature and combined) treatments, with the lowest value (14%) observed in the high temperature treatment. Comparatively, the percentage of total Chl-*a* in micro-phytoplankton was higher ($p < 0.05$, *t*-test) under rising pCO_2 when temperature was the same, with the highest value of 33.2% in the high CO_2 treatment. In contrast, the percentage of nano-phytoplankton increased under elevated temperature but decreased with rising pCO_2, with the highest value (81.4%) in the high temperature treatment and lowest percentage (64.0%) under high CO_2. The percentage of Chl-*a* biomass as pico-phytoplankton was small but showed a similar trend with that of the nano-phytoplankton, with the highest and lowest percentages of pico-phytoplankton being 4.6 and 2.8% under high temperature and high CO_2, respectively ($p < 0.05$, *t*-test, between the two treatments).

Species Composition of the Phytoplankton Assemblage

Microscopic cell counts indicated that the dominant phytoplankton group was diatoms throughout the time course of the incubation, with initial diatom and dinoflagellate abundances of 1090 cells L^{-1} and 300 cells L^{-1}, respectively. On the final sampling day, there were significant differences in the abundances of diatoms (**Figure 3A**) and dinoflagellates (**Figure 3B**) under different temperature and pCO_2 treatments. Diatom abundance was significantly lower (~0.5 fold, $p < 0.05$) in the high pCO_2 and combined treatments compared to the control ($4.518 \pm 0.468 \times 10^4$ cells L^{-1}) and high temperature treatments ($4.221 \pm 0.293 \times 10^4$ cells L^{-1}). However, at the same pCO_2 level, there was no significant difference between different temperature treatments ($p > 0.05$). The dinoflagellate abundance was highest in the high temperature treatment (1016 ± 155 cells L^{-1}, 5.6 fold of the control value). Compared to the control treatment (180 ± 122 cells L^{-1}, the abundance of dinoflagellates was also significantly higher in the high pCO_2 treatment (653 ± 151 cells L^{-1}). However, there was no significant difference between the control and combined treatments. The ratio of diatom to dinoflagellates abundances was highest at control (**Figure 3C**). The ratio significantly decreased by 89, 87, and 74% at high pCO_2, high temperature and combined treatments, respectively.

The species composition of the diatom community was also affected by the CO_2 and temperature treatments. The full list of diatom and dinoflagellate species and their abundances at the beginning and the four experimental treatments on the final sampling day of the incubation are listed in **Table 1**. The two most dominant diatom species at the beginning of the incubation were the centric species *Thalassiosira pacifica* (accounting for 55.91% of the total cell abundance on T0) and the pennate diatom

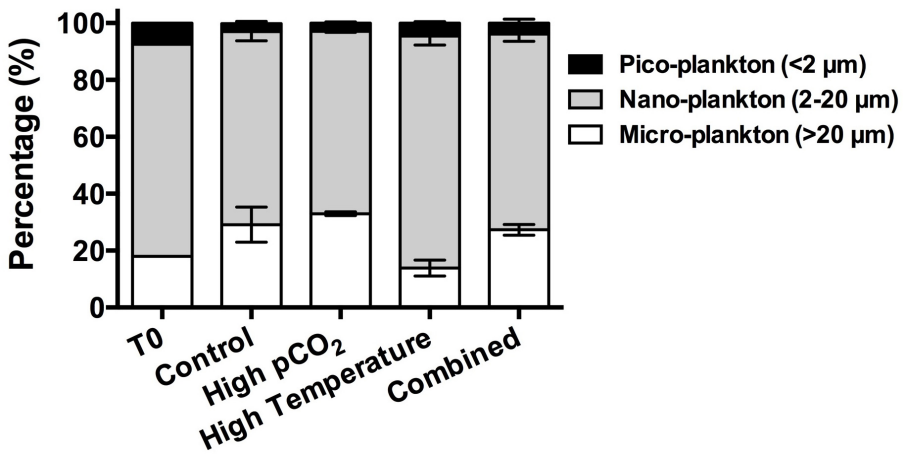

FIGURE 2 | Chl-*a* biomass percentages of micro-phytoplankton (>20 μm), nanoplankton (2–20 μm), and picoplankton (0.2–2 μm) in the beginning of the incubation (T0) and in the four experimental treatments on the final sampling day. Values are the means and error bars are the standard deviations of triplicates.

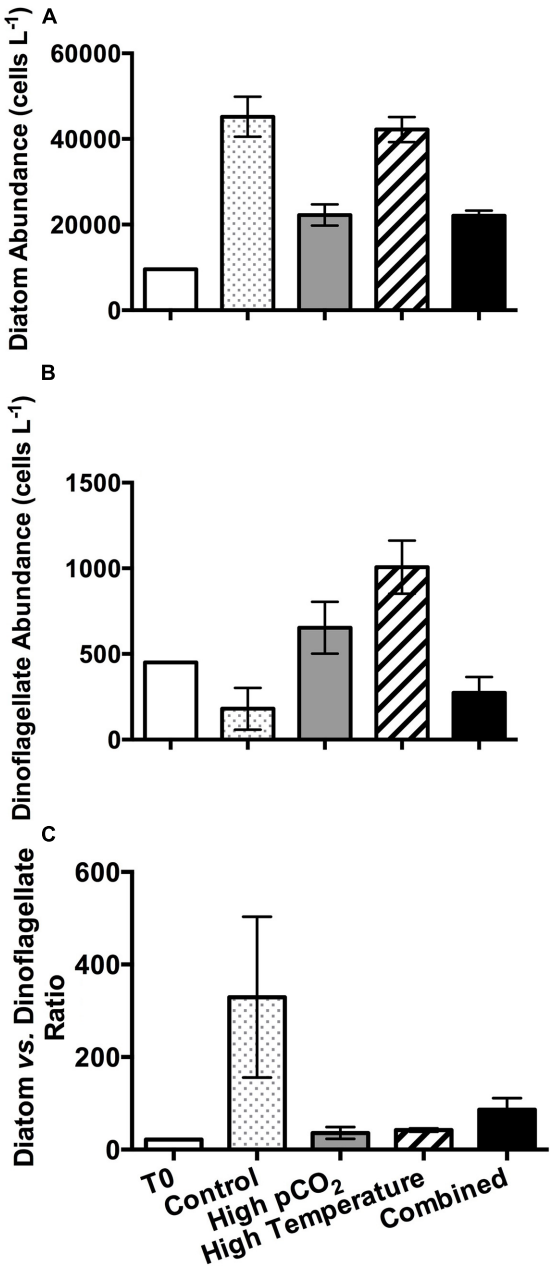

FIGURE 3 | Cell abundances of **(A)** diatoms and **(B)** dinoflagellates and **(C)** ratio of diatom to dinoflagellate abundances in the beginning of the incubation (T0) and in the four experimental treatments on the final sampling day. Values are the means and error bars are the standard deviations of triplicates.

Navicula sp. (18.12%). They continued to be the dominant centric and pennate diatom species respectively in the end of the incubation (**Table 1**). On the final sampling day, both the centric and pennate diatom abundances were significantly lower in the high pCO_2 and combined treatments, compared to the control and high temperature treatments (**Figure 4A**). The lowest abundance of centric diatoms was observed in the high pCO_2 treatment (0.57 fold of the control value), while the abundance of pennate diatoms was lowest in the combined treatment (10% of the control value). In contrast, the ratio of centric to pennate diatom abundance was significantly higher under the higher pCO_2 level, with the highest ratio of 9.8 ± 3.0 (ninefold of the control value) in the combined treatment (**Figure 4B**). Similarly, in the combined treatment, the abundance of the dominant centric diatom species *Thalassiosira pacifica* was highest, while that of the dominant pennate diatom species *Navicula* spp. was lowest among all the four experimental treatments (**Figure 4C**).

Elemental Composition and Community Sinking Rate

The average POC concentration was higher under higher pCO_2, especially with a significantly higher value in the combined treatment relative to the high temperature treatment (**Figure 5A**, $p < 0.05$). Similar to diatom concentration, the BSi concentrations were significantly lower in at higher pCO_2 when temperature was the same (**Figure 5B**, $p < 0.05$). Changing temperature alone had no significant effect on POC; while elevated temperature significantly increased BSi concentration at both pCO_2 levels ($p < 0.05$). The POP concentration was lowest (**Supplementary Data Sheet**) in the high pCO_2 treatment, with no significant difference among the other three treatments. However, there were no significant differences in PON concentrations in the four experimental treatments (**Supplementary Data Sheet**).

Both the POC to PON (C:N) and POC to POP (C:P) ratios were highest in the high pCO_2 treatment (**Figures 6A,B**); whereas there were no significant differences among the other three treatments (**Figures 6A,B**). Similarly, the POC to BSi (C:BSi) ratios were also significantly higher in the high pCO_2 and combined treatments compared to the control and high temperature treatments, with the highest ratio observed under high pCO_2 (25 ± 4, more than twofold of the control value, **Figure 6D**).

The sinking rate of the whole phytoplankton community was lowest in the combined treatment (0.12 ± 0.01 m d^{-1}, half of the control value), which coincided with the markedly higher centric:pennate diatom ratio in this treatment. However, there was no statistically significant difference among the other three treatments (**Figure 7**).

Individual and Interactive Effects of CO_2 and Temperature

The results of two-way ANOVA (**Table 2**) indicate that CO_2 had significant effects on most of the parameters sampled on the final sampling day, including the total diatom, centric diatom and pennate diatom abundances, ratios of diatom vs. dinoflagellate and centric vs. pennate abundances, POC and BSi concentrations, C:N, C:P, C:BSi and sinking rate of the community. Temperature had significant effects on dinoflagellate and pennate diatom abundances, ratios of diatom vs. dinoflagellate and centric vs. pennate abundances, BSi concentration and C:BSi.

For the two-way factorial interaction, CO_2 and temperature had significant interactive effects on the dinoflagellate and pennate diatom abundances, centric vs. pennate ratio and

TABLE 1 | List of all diatom and dinoflagellate species and the cell abundances (cells L^{-1}) identified with microscopy on T0 and the four experimental treatments on the final sampling day and cell volume of the dominant species.

Phytoplankton Species	Sampling Day and Treatments										Cell Volume
	T0		Control		High pCO_2		High Temperature		Combined		
	Cell Abundance	%	Cell Abundance	%	Cell Abundance	%	Cell Abundance	%	Cell Abundance	%	μm^3
Diatoms		95.7		99.7		97.1		97.6		98.7	
Centric Diatoms		70.3		50.6		60.1		53.8		88.6	
Thalassiosira pacifica	1.2×10^4	55.9	$(6.6 \pm 3.0) \times 10^3$	15.3	$(6.5 \pm 0.9) \times 10^3$	28.5	$(4.9 \pm 1.2) \times 10^3$	11.4	$(1.0 \pm 0.1) \times 10^4$	45.9	5655
Thalassiosira rotula	440	2.1	$(2.9 \pm 1.1) \times 10^3$	6.7	$(2.4 \pm 0.3) \times 10^3$	10.5			$(2.3 \pm 0.8) \times 10^3$	10.6	5741
Thalassiosira spp.					$(1.3 \pm 0.2) \times 10^3$	5.7	$(1.5 \pm 0.2) \times 10^3$	3.5	$(1.8 \pm 0.4) \times 10^3$	8.3	5842
Leptocylindrus danicus	690	3.3	$(6.1 \pm 0.4) \times 10^3$	14.1	$(1.4 \pm 0.4) \times 10^3$	6.1	$(4.8 \pm 1.2) \times 10^3$	11.2	$(1.4 \pm 0.5) \times 10^3$	6.4	
Paralia sulcata	520	2.5			293 ± 70	1.2	680 ± 140	1.6			
Climacodium biconcavum	460	2.2	$(2.9 \pm 0.2) \times 10^3$	6.7	307 ± 141	1.3	$(3.2 \pm 0.4) \times 10^3$	7.5	$(1.3 \pm 0.2) \times 10^3$	6.0	
Climacodium frauenfeldianum			273 ± 189	0.6					680 ± 330	3.1	
Ditylum brightwellii	420	2.0	$(1.4 \pm 0.1) \times 10^3$	3.2	253 ± 179	1.1	487 ± 94	1.1	233 ± 90	1.1	
Cyclotella striata	320	1.5	$(1.5 \pm 0.4) \times 10^3$	3.5	387 ± 90	1.7	$(3.7 \pm 0.8) \times 10^3$	8.6	$(1.0 \pm 0.2) \times 10^3$	4.6	
Guinardia delicatula	100	0.5	160 ± 53	0.4	393 ± 61	1.7	440 ± 60	1.0	260 ± 20	1.2	
Guinardia striata					460 ± 40	2.0	640 ± 72	1.5	260 ± 72	1.2	
Chaetoceros sp.	40	0.2							47 ± 30	0.2	
Coscinodiscus sp.	20	0.1	13 ± 23	0.03	34 ± 41	0.1	33 ± 42	0.1			
Detonula pumila							$(2.7 \pm 0.3) \times 10^3$	6.3			
Pennate Diatoms		25.4		49.1		37.0		43.8		10.1	
Navicula sp.	3.8×10^3	18.2	$(8.6 \pm 0.9) \times 10^3$	19.9	$(3.3 \pm 0.6) \times 10^3$	14.5	$(8.4 \pm 2.4) \times 10^3$	19.6	$(1.3 \pm 0.5) \times 10^3$	6.0	1500
Pinnularia spp.	680	3.3	$(5.6 \pm 2.8) \times 10^3$	13.0	$(3.1 \pm 1.2) \times 10^3$	13.6	$(4.4 \pm 0.6) \times 10^3$	10.3	420 ± 381	1.9	
Pseudonitzschia pungens	260	1.2	647 ± 179	1.5	$(1.3 \pm 0.1) \times 10^3$	5.7	640 ± 87	1.5			
Synedra sp.	240	1.2	113 ± 128	0.3	280 ± 87	1.2	360 ± 92	0.8	253 ± 42	1.2	
Nitzschia spp.	160	0.8	532 ± 61	1.2			460 ± 156	1.1			
Nitzschia longissima	80	0.4	$(5.7 \pm 3.8) \times 10^3$	13.2	460 ± 69	2.0	$(4.2 \pm 1.0) \times 10^3$	9.8	220 ± 104	1.0	
Pleurosigma sp.	60	0.3									
Thalassiothrix longissima							340 ± 69	0.8			
Dinoflagellates		4.3		0.3		2.9		2.4		1.3	
Gymnodinium sp.	460	2.2	146 ± 155	0.3	240 ± 20	1.1	326 ± 61	0.8	73 ± 11	0.3	
Oxytoxum parvum	400	1.9			260 ± 72	1.1	680 ± 171	1.6	220 ± 80	1.0	
Podolampas palmipes	40	0.2			153 ± 99	0.7					

The errors are the standard deviations of the triplicate values. The percentage values were calculated based on the average abundance of the triplicate samples.

C:P (**Table 2**). Among these two-way interactive effects, CO_2 and temperature interaction had antagonistic effects on the dinoflagellate abundance, diatom vs. dinoflagellate ratio and C:P, but synergistic effects on the pennate diatom abundance and centric vs. pennate ratio.

DISCUSSION

This study reveals that phytoplankton community size and species composition, elemental ratios, and the sinking rate of the phytoplankton community collected from the Tianjin coastal area all responded to increased pCO_2 and/or warming. Apart from the individual effects, the interaction of CO_2 and temperature had significant interactive effects on some of the examined parameters, thus having implications for marine biogeochemistry in the future environment. It is noteworthy that our continuous incubation experiment is different from the commonly used short-term batch/grow-out culture technique. This continuous incubation method allows the acclimation of the natural phytoplankton assemblage to the experimental conditions for a much longer period of time (21 days in our study). Community changes in a continuous culture system reflect differences in the growth rates of individual phytoplankton species under the experimental conditions, as faster-growing species come to dominate the assemblage

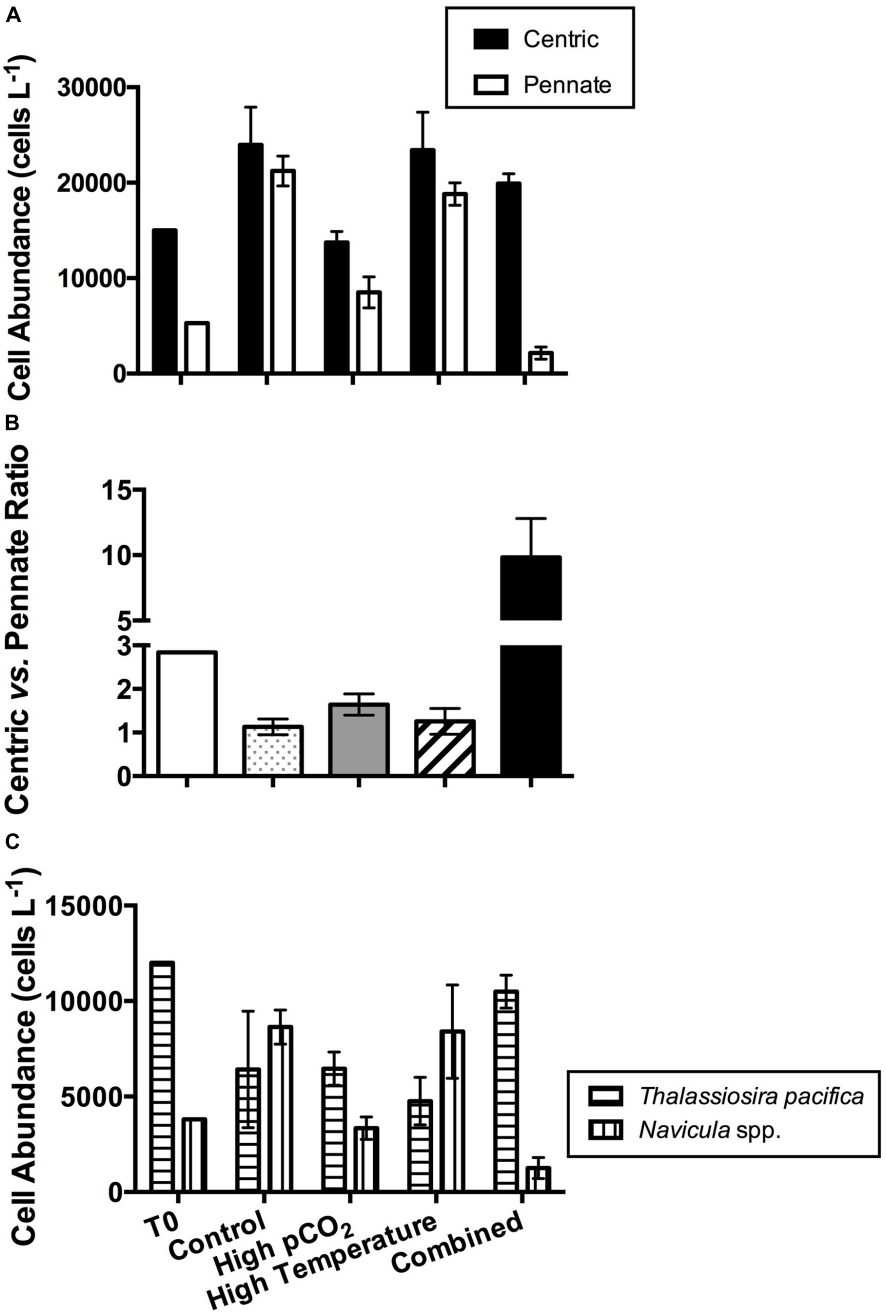

FIGURE 4 | Diatom assemblage composition in the four experimental treatments in the beginning of the incubation (T0) and on the final sampling day: **(A)** cell abundances of centric and pennate diatoms; **(B)** ratio of centric diatom to pennate diatom cell abundances; **(C)** cell abundances of dominant diatom species. Values are the means and error bars are the standard deviations of triplicates.

while slower-growing species are 'washed out' by dilution. In addition, nutrient enrichment, the "bottle effects" and excluding the large grazers may favor certain phytoplankton groups such as diatoms (Buma et al., 1991; Litchman et al., 2007), as suggested by the differences in the sampled parameters between T_0 and T_{final} in our study. Nevertheless, it allows our final sampling to reflect the responses of the natural phytoplankton community to the environmental changes under a relatively steady growth phase (Hutchins et al., 2003; Feng et al., 2009).

Phytoplankton Community Size Structure

The total phytoplankton Chl-*a* biomass was significantly promoted by warming, especially during the batch growth

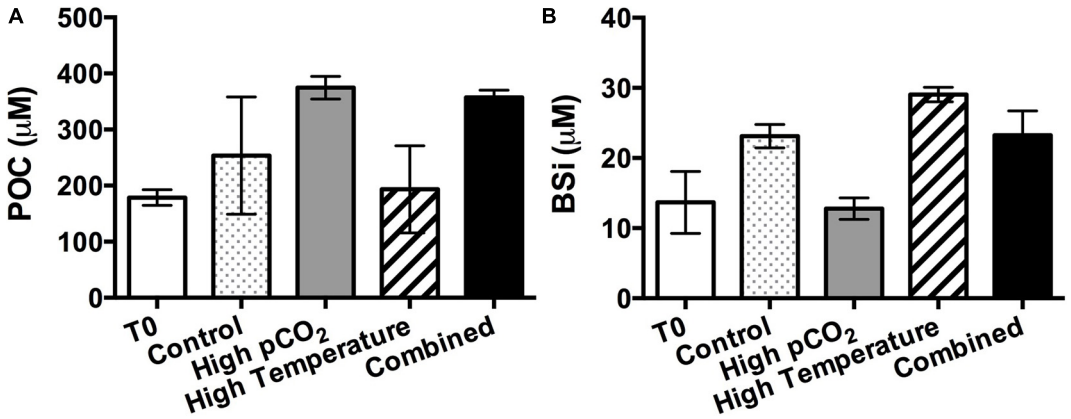

FIGURE 5 | Particulate organic carbon (POC, **A**) and biogenic silica (BSi, **B**) concentrations in the beginning of the incubation (T0) and in the four experimental treatments on the final sampling day. Values are the means and error bars are the standard deviations of triplicates.

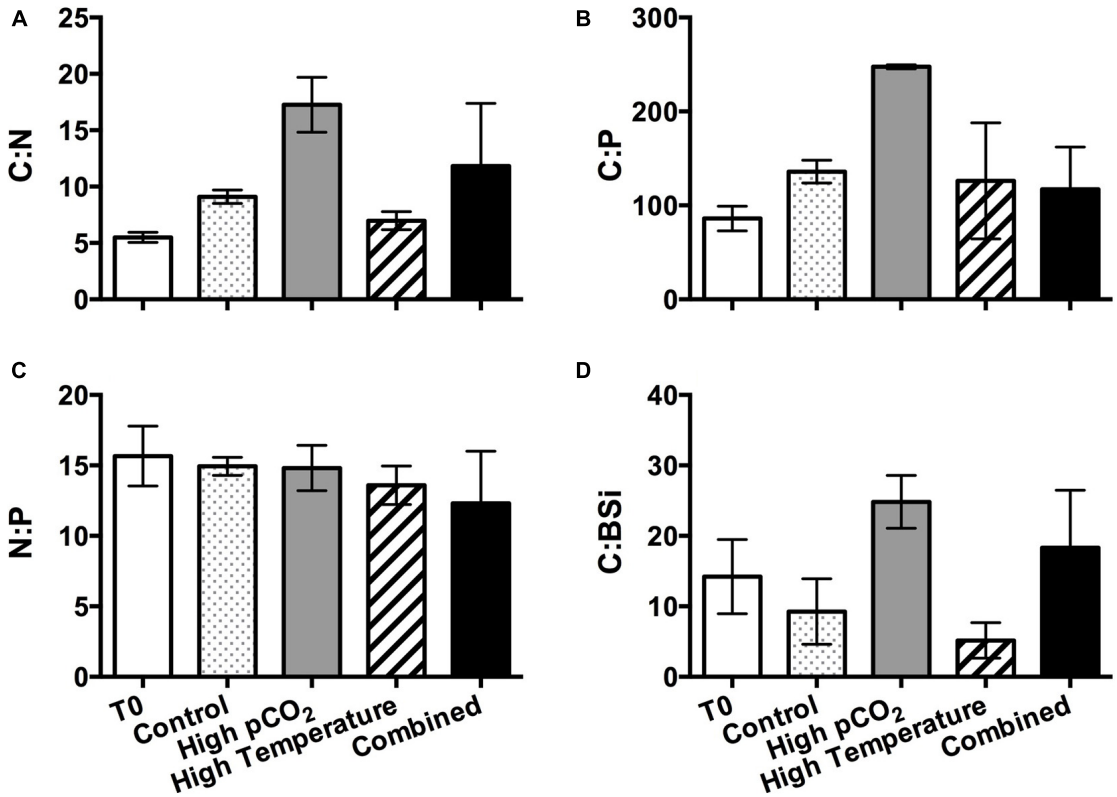

FIGURE 6 | Elemental molar ratios in the beginning of the incubation (T0) and in the four experimental treatments on the final sampling day: **(A)** particulate organic carbon to particulate organic nitrogen ratio (C:N); **(B)** particulate organic carbon to particulate organic phosphorus ratio (C:P); **(C)** particulate organic nitrogen to particulate organic phosphorus ratio (N:P); and **(D)** particulate organic carbon to biogenic silica ratio (C:BSi). Values are the means and error bars are the standard deviations of triplicates.

mode in the first few days with higher values in the high temperature and combined treatments (**Figure 1**). This warming effect is similar to some previous studies on spring phytoplankton assemblages in both coastal regions (Lee et al., 2019) and the open ocean (Feng et al., 2009), mainly due to the thermal stimulation of phytoplankton metabolism within a favorable temperature range (Eppley, 1972). However, a mesocosm study using a phytoplankton assemblage in the coastal Kiel Fjord showed an opposite trend of decreased Chl-*a* biomass under warming, mainly due to the fact that temperature increases of 6°C promoted zooplankton grazing more than phytoplankton growth (Sommer et al., 2015). In our study, however, we deliberately

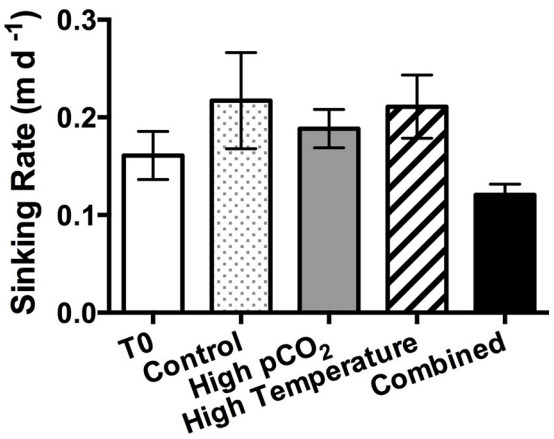

FIGURE 7 | Sinking rates of the phytoplankton community in the beginning of the incubation (T0) and in the four experimental treatments on the final sampling day. Values are the means and error bars are the standard deviations of triplicates.

removed or reduced larger zooplankton numbers at the outset of the study using a coarse mesh screen, yielding much weakened grazing pressure on the phytoplankton biomass, with only few microzooplankton cells detected in the T0 samples. The removal of large grazers, together with the nutrient enrichment, also resulted in the rapid increase in the total Chl-*a* concentration in all the incubation bottles during the batch growth mode.

Size-fractionated Chl-*a* biomass changes suggested that the size of the phytoplankton assemblage may be affected by both temperature and pCO_2. Warming greatly reduced the relative biomass percentage of larger micro-plankton cells, while increasing the nano-plankton and pico-plankton percentages (**Figure 2**). This trend is consistent with some previously published results, showing that elevated temperature may favor smaller species in competition at the community level (Hare et al., 2007a; Daufresne et al., 2009), or simply decrease the cell-size of some species when they grow faster (Atkinson et al., 2003; Sheridan and Bickford, 2011). On the other hand, the larger cell (>20 μm) contribution to total Chl-*a* biomass was increased by CO_2 enrichment under both temperature conditions in our study, and yielded the highest relative abundance of micro-plankton in the high pCO_2 treatment. There is no compelling evidence of CO_2 effects on cell size within individual species (reviewed by Finkel et al., 2010). Therefore, the changes in community size structure were mainly caused by shifts in phytoplankton species, in agreement with a previous study conducted off the coast of Norway (Engel et al., 2008). Compared to small phytoplankton cells, the growth of larger phytoplankton species tends to be more favored by CO_2 enrichment, mainly due to differences in CCM and/or diffusion boundary layer thicknesses (Raven et al., 2008; Finkel et al., 2010).

Phytoplankton Dominance Shifts

Along with the effects of CO_2 and warming on the size structure of the phytoplankton assemblage, changes in CO_2/temperature also caused shifts in the taxonomic composition of the phytoplankton assemblage in our study. Due to the constraints of the microscopic method that small phytoplankton cells (<5 μm) are harder to be distinguished, the species determined here mostly belonged to the micro-plankton and nano-plankton groups. Here we observed that the abundance of dinoflagellates was especially promoted in the high temperature treatment (**Figure 3B**). Although diatoms generally grow much faster than dinoflagellates at the same temperature (Chen and Laws, 2017), the distribution of many dinoflagellate species tends to be more favored in warm waters, compared to diatoms (Finkel et al., 2010; Xiao et al., 2018). Nevertheless,

TABLE 2 | The individual and multiplicative effects of temperature and CO_2 and types of driver interactions on the parameters of the final sampling day of the experiment.

Parameter	CO_2	Temperature	Interaction	Individual effect (%)		Multiplicative effect (%)		Type of interaction
				CO_2	Temperature	Observed	Calculated	
Diatom abundance	*	–	–	–51				
Dinoflagellate abundance	–	*	*	262	459	52	1929	Antagonism
Diatoms vs. dinoflagellates	*	*	*	–89	–87	–74	–99	Antagonism
Centric diatom abundance	*	–	–	–43				
Pennate diatom abundance	*	*	*	–60	–11	–90	–64	Synergism
Centric vs. pennate	*	*	*	45	11	769	61	Synergism
POC concentration	*	–	–	48				
BSi concentration	*	*	–	–45	26			
N:P	–	–	–					
C:N	*	–	–	–45				
C:P	*	–	*	82	–7	–14	69	Antagonism
C:BSi	*	*	–	205	–44			
Sinking rate	*	–	–	–13				

"" represents significance and "–" represents non-significance at the p = 0.05 level using two-way ANOVA test.*
Individual/multiplicative effect was only calculated when there was statistical significance. Types of interaction were only determined for the parameters that CO_2 and temperature had significant interactive effects on. The full two-way ANOVA results can be found in ***Supplementary Table S2****.*

dinoflagellate abundance decreased again in the combined treatment, likely due to the outcome of competition with other nano-phytoplankton and pico-plankton groups. In coastal regions, diatoms and dinoflagellates are the major dominating phytoplankton functional groups (Smayda and Reynolds, 2003). The ratio of diatoms to dinoflagellates is considered to be an environmental indicator, with higher diatoms: dinoflagellates values indicating better seawater quality (Wasmund et al., 2017) and alleviating the eutrophication problem of the water column (Spilling et al., 2018). Changes in phytoplankton species composition may affect the food quality provided to the upper food web (Rose et al., 2009) and reproduction of the zooplankton, with higher copepod reproduction related to relative higher dinoflagellates abundance (Vehmaa et al., 2011). In addition, during costal spring blooms with low grazing pressure, sinking of ungrazed phytoplankton cells contributes to the bottom hypoxia. Diatom cells tend to sink out of the surface layer faster than dinoflagellates and these generally larger cells consume more oxygen during degradation in the subsurface waters; hence, decrease in diatom abundance likely results in reduced oxygen demand of the bottom water in the coastal regions (Spilling and Lindström, 2008). Our results suggest that the proportion of diatoms to dinoflagellates significantly decreased when either pCO_2 or temperature was increased individually or simultaneously, indicating a potential negative feedback of future climate change on the oxygen demand in bottom waters in the Bohai Bay area, as demonstrated for the Baltic Sea (Wasmund et al., 2017).

Both diatom abundance and species composition was significantly affected by changes in pCO_2 (**Figure 3A**). The diatom RubisCO enzyme tends to have a high affinity for CO_2, supplied by efficient CCMs (Gao and Campbell, 2014), and thus diatom photosynthesis may be already saturated under present day CO_2 conditions (Burkhardt et al., 2001; Rost et al., 2003). As a result, although diatoms were still dominant in the phytoplankton assemblage, total diatom abundance as well as centric and pennate diatom abundances were not promoted, but rather all decreased at higher pCO_2 in our study (**Figure 4**). This is most likely due to the outcome of the competition with other phytoplankton groups that were favored more under higher pCO_2. Similarly, a study on the South China Sea phytoplankton community also found diatom abundance declined with elevated CO_2 (Gao et al., 2012). However, the abundance of the dominant centric diatom species *T. pacifica* and the centric vs. pennate diatom ratio showed an opposite trend in our study. The higher centric vs. pennate diatom ratio observed in our study is consistent with previous findings of CO_2 enrichment experiments on the Southern Ocean phytoplankton community, which also reported larger centric diatoms were favored more under rising pCO_2 (Tortell et al., 2008; Feng et al., 2010), further indicating differential responses to CO_2 among different diatom taxonomic groups (Wu et al., 2014). By synthesizing the results of more than a decade research on natural diatom communities responses to OA, Bach and Taucher (2019) also found that more than 65% of the experiments showed changes in diatom species composition with a trend of shifting toward larger species. The taxonomic changes toward larger cells may in turn accelerate the energy transfer efficiency into higher trophic levels in marine food web (Bach and Taucher, 2019). In our study, the centric vs. pennate diatom ratio was further increased in the combined treatment, suggesting potential further influence on the energy transfer in the food web of Bohai Bay area in the future climate change scenario.

Elemental Stoichiometry and Sinking Rate

As a consequence of the shifts in phytoplankton species composition and the direct intra-specific physiological responses to the experimental conditions under different temperature and CO_2 levels, our results also showed significant changes in the elemental composition (POC and BSi concentrations, C:N, C:P, and C:BSi, **Figure 6**) of the phytoplankton community. The significantly higher C:N and C:P ratios in the high pCO_2 treatment were consistent with the results of previous laboratory studies on phytoplankton, including isolates of cyanobacteria (Fu et al., 2007), coccolithophores (Feng et al., 2008), and diatoms (Burkhardt and Riebesell, 1997). This finding likely indicates that CO_2 enrichment promotes carbon fixation more than N and P uptake, and may further have implications on predicting the elemental stoichiometry of the organic matter export by marine phytoplankton into the deeper layers. Nevertheless, Taucher et al. (2020) synthesized the data of *in situ* manipulation experiments on natural plankton community and observed OA-induced 20% increase to 17% decrease in C:N export ratio in the sinking particles. Their results also suggest the C:N export ratio can be regulated greatly by plankton feeding and microbial degradation, as well as other environmental drivers such as temperature and nutrient availability (Taucher et al., 2020 and references therein).

Another significant trend was the increased C:BSi ratios under CO_2 enrichment mainly caused by enhanced POC accumulation and reduced BSi concentration under higher pCO_2. The latter may be attributed not only to reduced total diatom abundance, but also to decreased BSi production by diatoms. Milligan et al. (2004) reported enhanced efflux of silicate from the diatom cells at high pCO_2 while silicate influx was not changed; as a result, the cellular silica quota was reduced with elevated pCO_2 (Milligan et al., 2004). A study on a Southern Ocean diatom assemblage also found decreased community silica production under seawater acidification, but with strain-specific responses (Petrou et al., 2019). In general, mean silica production has a linear relationship with the surface area of diatom cells (McNair et al., 2018), but is not necessarily correlated with the growth rate (Petrou et al., 2019). However, the complete mechanisms of CO_2 regulation of BSi production are still not clearly understood. The silica cell walls of diatoms are considered in the context of functions that include defense from grazing (Hamm et al., 2003) and ballast for sinking and carbon export (Buesseler, 1998). As such, further understanding the regulatory mechanisms for BSi production in the changing marine environment will help to unravel the impacts of environmental changes on carbon export in diatom-dominated waters.

In our study, the sinking rate of the phytoplankton assemblage was lowest in the combined treatment, mainly affected by pCO_2

based on the two-way ANOVA results, despite the lowest BSi concentration being observed in the high pCO_2 treatment. Although the ballasting effect of BSi is an important factor driving the sinking rate of diatoms, the reduced sinking rate in the combined treatment might be attributed to the changes in phytoplankton species composition instead. Compared to the other three experimental treatments, the abundance of the dominant centric diatom species *T. pacifica* was remarkably higher in the combined treatment (**Table 1** and **Figure 4C**). It is noteworthy that *T. pacifica* is a chain-forming species, and the formation of chains can influence buoyancy and slow the sinking rates of the cells (Smayda and Boleyn, 1966). On top of that, the chain length of the chain-forming diatoms tends to increase with rising pCO_2 as in the case of *Asterionellopsis glacialis* (Barcelos e Ramos et al., 2014), while the size of the phytoplankton community may be decreased under elevated temperature, together further reducing the sinking rate in the combined treatment (Denny, 1993). The sinking rate of a phytoplankton community can also be affected the production of transparent exopolymer particles (TEP), which have lower density but facilitate the cells to form large aggregates (Alldredge and Jackson, 1995). As the carbon production in the surface layer is the major contributor of carbon export to depth (Tréguer et al., 2018), if our finding represents a general future trend, OA and warming together may weaken carbon export from the surface layer in diatom-dominated coastal environments. However, we also should consider that, in the real oceanic environment, the actual carbon export to depth will generally be further influenced by grazing and remineralization processes (Armstrong et al., 2002).

Driver Interactions and Implications for the Coastal Biogeochemistry Under Global Change

The findings of our study suggest that both the individual and interactive effects of OA and warming are important to consider for coastal phytoplankton assemblages. There is clear evidence that many environmental drivers are already changing simultaneously in coastal and oceanic regions, including ocean acidification, warming, deoxygenation, changes in nutrient supply, and surface irradiance regimes (IPCC, 2014; Hutchins and Fu, 2017). Therefore, it is urgent to understand the cumulative effects of multiple drivers on the marine biota, and disentangle the interactive patterns of these drivers (Boyd et al., 2018). Our results suggest that CO_2 and temperature synergistically affected pennate diatom abundance and the centric vs. pennate diatom ratio, and had antagonistic effects on dinoflagellate abundance and the ratio of diatom:dinoflagellate abundances. The cumulative effects of OA and warming together may either "amplify" or "shrink" the effects of the individual-driver effects, further emphasizing the importance of considering multiple driver interactions for predicting the biogeochemical responses to future environmental changes. Similarly, a study on the South China Sea phytoplankton community observed that although OA and warming alone promoted the phytoplankton productivity, the combination of the two drivers had an antagonistic effect (Zhang et al., 2018). Sett et al. (2018) also reported strongly shifted diatom species composition by the combined effect of OA and warming. During the past decade, many studies have focused on examining the combined effects of OA and other environmental drivers on natural phytoplankton community (Bach and Taucher, 2019 and references therein). Future work also needs to compile the published results and synthesize the general patterns of the interactive effects of OA and warming on natural phytoplankton assemblages in different oceanic regions.

Overall, our study on a spring bloom phytoplankton assemblage reveals that under future environmental conditions when both OA and warming effects are considered, the centric to pennate diatom ratio will increase, while the diatom:dinoflagellate ratio and phytoplankton-induced sinking rate will significantly decrease in the coastal Bohai Bay area. These changes may further impact carbon export and elemental cycles in the coastal ecosystem, and may impact food and nutritional availability to higher trophic levels, thus affecting coastal fisheries. However, there are limitations to how far we can extrapolate our findings. Our study examined CO_2 and warming effects using a coastal phytoplankton assemblage acclimated to constant experimental conditions. In contrast, CO_2/temperature variability is generally high in the coastal environment (Dai et al., 2009; Li et al., 2016; Kling et al., 2020), especially in regions highly influenced by anthropogenic activities like Bohai Bay. Consequently, coastal phytoplankton assemblages may possess relatively high tolerance limits to thermal and CO_2 shifts. Future studies are needed that examine the effects of ocean acidification and warming in the context of natural fluctuations in pCO_2 and temperature in coastal ecosystems.

DATA AVAILABILITY STATEMENT

The original contributions presented in the study are included in the article/**Supplementary Material**, further inquiries can be directed to the corresponding author/s.

AUTHOR CONTRIBUTIONS

YF designed the study. YL, PL, and TZ conducted the experiments. YL, PL, TZ, TC, and FF analyzed the samples. YF, FC, MW, FF, and DH thoroughly discussed the results and interpreted the data. YF, FC, MW, and DH wrote the manuscript with contributions from all co-authors. All the authors contributed to the article and approved the submitted version.

FUNDING

This work was supported by the National Natural Science Foundation of China grants (nos. 41676160 and 41306118), the Tianjin Natural Science Foundation (19JCYBJC22900), Tianjin Municipal Education Commission Project (2017KJ014), and the open fund of State Key Laboratory of Satellite Ocean

Environment Dynamics, Second Institute of Oceanography (QNHX1803) to YF, and US National Science Foundation grants (OCE 1638804 and OCE 1851222) to DH.

ACKNOWLEDGMENTS

We would like to thank undergraduate students Dandan Hou, Meiqi Li, and Wenzhang Feng at Tianjin University of Science and Technology for helping with seawater collection and experimental setup. We also thank Dr. Guisheng Song's laboratory at Tianjin University for analyzing the dissolved inorganic carbon concentration.

SUPPLEMENTARY MATERIAL

The Supplementary Material for this article can be found online at: https://www.frontiersin.org/articles/10.3389/fmars.2021.622319/full#supplementary-material

REFERENCES

Alldredge, A. L., and Jackson, G. A. (1995). Aggregation in marine systems — preface. *Deep Sea Res. II* 42, 1–7. doi: 10.1016/s0924-7963(02)00049-0

Armstrong, R. A., Lee, C., Hedges, J. I., Honjo, S., and Wakeham, S. G. (2002). A new mechanistic model for organic carbon fluxes in the ocean based on the quantitative association of POC with ballast minerals. *Deep Sea Res. II* 49, 219–236. doi: 10.1016/s0967-0645(01)00101-1

Atkinson, D., Ciotti, B. J., and Montagnes, D. J. S. (2003). Protists decrease in size linearly with temperature: CA. 2.5% degrees C-1. *Proc. R. Soc. B Biol. Sci.* 270, 2605–2611. doi: 10.1098/rspb.2003.2538

Bach, L. T., and Taucher, J. (2019). CO_2 effects on diatoms: a synthesis of more than a decade of ocean acidification experiments with natural communities. *Ocean Sci.* 15, 1159–1175. doi: 10.5194/os-15-1159-2019

Barcelos e Ramos, J., Schulz, K. G., Brownlee, C., Sett, S., and Azevedo, E. B. (2014). Effects of increasing seawater carbon dioxide concentrations on chain formation of the diatom *Asterionellopsis glacialis*. *PLoS One* 9:e90749. doi: 10.1371/journal.pone.0090749

Beaufort, L., Probert, I., de Garidel-Thoron, T., Bendif, E. M., Ruiz-Pino, D., Metzl, N., et al. (2011). Sensitivity of coccolithophores to carbonate chemistry and ocean acidification. *Nature* 476, 80–83. doi: 10.1038/nature10295

Bienfang, P. K. (1981). SETCOL—a technologically simple and reliable method for measuring phytoplankton sinking rates. *Can. J. Fishe. Aquat. Sci.* 38, 1289–1294. doi: 10.1139/f81-173

Bopp, L., Resplandy, L., Orr, J. C., Doney, S. C., Dunne, J. P., Gehlen, M., et al. (2013). Multiple stressors of ocean ecosystems in the 21st century: projections with CMIP5 models. *Biogeosciences* 10, 6225–6245. doi: 10.5194/bg-10-6225-2013

Boyd, P. W., Collins, S., Dupont, S., Fabricius, K., Gattuso, J. P., Havenhand, J., et al. (2018). Experimental strategies to assess the biological ramifications of multiple drivers of global ocean change—a review. *Glob. Chang. Biol.* 24, 2239–2261. doi: 10.1111/gcb.14102

Boyd, P. W., and Hutchins, D. A. (2012). Understanding the responses of ocean biota to a complex matrix of cumulative anthropogenic change. *Mar. Ecol. Prog. Ser.* 470, 125–135. doi: 10.3354/meps10121

Brzezinski, M. A., and Nelson, D. M. (1995). The annual silica cycle in the Sargasso Sea near Bermuda. *Deep Sea Res. Part I Oceanogr. Res. Pap.* 42, 1215–1237. doi: 10.1016/0967-0637(95)93592-3

Buesseler, K. O. (1998). The decoupling of production and particulate export in the surface ocean. *Glob. Biogeochemi. Cycles* 12, 297–310. doi: 10.1029/97gb03366

Buma, A. G., De Baar, H. J., Nolting, R. F., and Van Bennekom, A. J. (1991). Metal enrichment experiments in the Weddell—Scotia Seas: effects of iron and manganese on various plankton communities. *Limnol. Oceanogr.* 36, 1865–1878. doi: 10.4319/lo.1991.36.8.1865

Burkhardt, S., Amoroso, G., Riebesell, U., and Sultemeyer, D. (2001). CO_2 and HCO_3^- uptake in marine diatoms acclimated to different CO_2 concentrations. *Limnol. Oceanogr.* 46, 1378–1391. doi: 10.4319/lo.2001.46.6.1378

Burkhardt, S., and Riebesell, U. (1997). CO_2 availability affects elemental composition (C: N: P) of the marine diatom *Skeletonema costatum*. *Mar. Ecol. Prog. Ser.* 155, 67–76. doi: 10.3354/meps155067

Burkhardt, S., Zondervan, I., and Riebesell, U. (1999). Effect of CO_2 concentration on C: N: P ratio in marine phytoplankton: a species comparison. *Limnol. Oceanogr.* 44, 683–690. doi: 10.4319/lo.1999.44.3.0683

Cai, W.-J., Hu, X., Huang, W.-J., Murrell, M. C., Lehrter, J. C., Lohrenz, S. E., et al. (2011). Acidification of subsurface coastal waters enhanced by eutrophication. *Nat. Geosci.* 4, 766–770. doi: 10.1038/ngeo1297

Caldeira, K., and Wickett, M. E. (2003). Anthropogenic carbon and ocean pH. *Nature* 425, 365–365. doi: 10.1038/425365a

Carton, J. A., and Giese, B. S. (2008). A reanalysis of ocean climate using simple ocean data assimilation (SODA). *Mon. Weather Rev.* 136, 2999–3017. doi: 10.1175/2007mwr1978.1

Chen, B., and Laws, E. A. (2017). Is there a difference of temperature sensitivity between marine phytoplankton and heterotrophs? *Limnol. Oceanogr.* 62, 806–817. doi: 10.1002/lno.10462

Dai, M., Lu, Z., Zhai, W., Chen, B., Cao, Z., Zhou, K., et al. (2009). Diurnal variations of surface seawater pCO_2 in contrasting coastal environments. *Limnol. Oceanogr.* 54, 735–745. doi: 10.4319/lo.2009.54.3.0735

Daufresne, M., Lengfellner, K., and Sommer, U. (2009). Global warming benefits the small in aquatic ecosystems. *Proc. Natl. Acad. Sci. U.S.A.* 106, 12788–12793. doi: 10.1073/pnas.0902080106

Denny, M. (1993). *Air and Water: The Biology and Physics of Life's Media*. Princeton, NJ: Princeton University Press.

Dickson, A. G., and Millero, F. J. (1987). A comparison of the equilibrium-constants for the dissociation of carbonic-acid in seawater media. *Deep Sea Res. Part A Oceanogr. Res. Pap.* 34, 1733–1743. doi: 10.1016/0198-0149(87)90021-5

Dickson, A. G., Sabine, C. L., and Christian, J. R. (2007). *Guide to Best Practices for Ocean CO_2 Measurements*. Sidney, BC: North Pacific Marine Science Organization.

Engel, A., Schulz, K. G., Riebesell, U., Bellerby, R., Delille, B., and Schartau, M. (2008). Effects of CO_2 on particle size distribution and phytoplankton abundance during a mesocosm bloom experiment (PeECE II). *Biogeosciences* 5, 509–521. doi: 10.5194/bg-5-509-2008

Eppley, R. W. (1972). Temperature and phytoplankton growth in the sea. *Fish. Bull.* 70, 1063–1085.

Falkowski, P. G., and Raven, J. A. (2007). *Aquatic Photosynthesis*. Princeton, NJ: Princeton University Press.

Feely, R. A., Doney, S. C., and Cooley, S. R. (2009). Ocean acidification: present conditions and future changes in a high-CO_2 world. *Oceanography* 22, 36–47. doi: 10.5670/oceanog.2009.95

Feng, L., and Lin, X.-P. (2009). Long-term trend of the east china sea surface temperature during 1945˜ 2006. *Period. Ocean Univ. China* 39, 13–18. (In Chinese with English abstract),

Feng, Y., Hare, C. E., Leblanc, K., Rose, J. M., Zhang, Y. H., Ditullio, G. R., et al. (2009). Effects of increased pCO_2 and temperature on the North Atlantic spring bloom. I. The phytoplankton community and biogeochemical response. *Mar. Ecol. Prog. Ser.* 388, 13–25. doi: 10.3354/meps08133

Feng, Y., Hare, C. E., Rose, J. M., Handy, S. M., Ditullio, G. R., Lee, P. A., et al. (2010). Interactive effects of iron, irradiance and CO_2 on Ross Sea phytoplankton. *Deep Sea Res. Part I Oceanogr. Res. Pap.* 57, 368–383. doi: 10.1016/j.dsr.2009.10.013

Feng, Y., Roleda, M. Y., Armstrong, E., Summerfield, T. A., Law, C. S., Hurd, C. L., et al. (2020). Effects of multiple drivers of ocean global change on the physiology and functional gene expression of the coccolithophore *Emiliania huxleyi*. *Glob. Chang. Biol.* 26, 5630–5645. doi: 10.1111/gcb.15259

Feng, Y., Warner, M. E., Zhang, Y., Sun, J., Fu, F. X., Rose, J. M., et al. (2008). Interactive effects of increased pCO_2, temperature and irradiance on the marine

coccolithophore *Emiliania huxleyi* (Prymnesiophyceae). *Eur. J. Phycol.* 43, 87–98. doi: 10.1080/09670260701664674

Finkel, Z. V., Beardall, J., Flynn, K. J., Quigg, A., Rees, T. A. V., and Raven, J. A. (2010). Phytoplankton in a changing world: cell size and elemental stoichiometry. *J. Plankton Res.* 32, 119–137. doi: 10.1093/plankt/fbp098

Fitzer, S. C., Torres Gabarda, S., Daly, L., Hughes, B., Dove, M., O'connor, W., et al. (2018). Coastal acidification impacts on shell mineral structure of bivalve mollusks. *Ecol. Evol.* 8, 8973–8984. doi: 10.1002/ece3.4416

Folt, C. L., Chen, C. Y., Moore, M. V., and Burnaford, J. (1999). Synergism and antagonism among multiple stressors. *Limnol. Oceanogr.* 44, 864–877. doi: 10.4319/lo.1999.44.3_part_2.0864

Fu, F. X., Warner, M. E., Zhang, Y. H., Feng, Y. Y., and Hutchins, D. A. (2007). Effects of increased temperature and CO_2 on photosynthesis, growth, and elemental ratios in marine *Synechococcus* and *Prochlorococcus* (Cyanobacteria). *J. Phycol.* 43, 485–496. doi: 10.1111/j.1529-8817.2007.00355.x

Gao, K., and Campbell, D. A. (2014). Photophysiological responses of marine diatoms to elevated CO_2 and decreased pH: a review. *Funct. Plant Biol.* 41, 449–459. doi: 10.1071/fp13247

Gao, K., Xu, J., Gao, G., Li, Y., Hutchins, D. A., Huang, B., et al. (2012). Rising CO_2 and increased light exposure synergistically reduce marine primary productivity. *Nat. Clim. Chang.* 2, 519–523. doi: 10.1038/nclimate1507

Hamm, C. E., Merkel, R., Springer, O., Jurkojc, P., Maier, C., Prechtel, K., et al. (2003). Architecture and material properties of diatom shells provide effective mechanical protection. *Nature* 421, 841–843. doi: 10.1038/nature01416

Hare, C. E., DiTullio, G. R., Riseman, S. F., Crossley, A. C., Popels, L. C., Sedwick, P. N., et al. (2007a). Effects of changing continuous iron input rates on a Southern Ocean algal assemblage. *Deep Sea Res. I* 54, 732–746. doi: 10.1016/j.dsr.2007.02.001

Hare, C. E., DiTullio, G. R., Trick, C. G., Wilhelm, S. W., Bruland, K. W., Rue, E. L., et al. (2005). Phytoplankton community structure changes following simulated upwelled iron inputs in the Peru Upwelling region. *Aquat. Microb. Ecol.* 38, 269–282. doi: 10.3354/ame038269

Hare, C. E., Leblanc, K., Ditullio, G. R., Kudela, R. M., Zhang, Y., Lee, P. A., et al. (2007b). Consequences of increased temperature and CO_2 for phytoplankton community structure in the Bering Sea. *Mar. Ecol. Prog. Ser.* 352, 9–16. doi: 10.3354/meps07182

Hutchins, D. A., and Fu, F. X. (2017). Microorganisms and ocean global change. *Nat. Microbiol.* 2:17508. doi: 10.1038/nmicrobiol.2017.58

Hutchins, D. A., Fu, F. X., Warner, M. E., Feng, Y., Portune, K., Bernhardt, P. W., et al. (2007). CO_2 control of *Trichodesmium* N_2 fixation, photosynthesis, growth rates, and elemental ratios: implications for past, present, and future ocean biogeochemistry. *Limnol. Oceanogr.* 52, 1293–1340. doi: 10.4319/lo.2007.52.4.1293

Hutchins, D. A., Mulholland, M. R., and Fu, F. X. (2009). Nutrient cycles and marine microbes in a CO_2-enriched ocean. *Oceanography* 22, 128–145. doi: 10.5670/oceanog.2009.103

Hutchins, D. A., Pustizzi, F., Hare, C. E., and Ditullio, G. R. (2003). A shipboard natural community continuous culture system for ecologically relevant low-level nutrient enrichment experiments. *Limnol. Oceanogr. Methods* 1, 82–91. doi: 10.4319/lom.2011.1.82

IPCC (2014). *Climate Change 2014: Synthesis Report. Contribution of Working Groups I, II and II to the FIfth Assessment Report of the Intergovernmental Panel on Climate Change*. Geneva: IPCC.

Joint, I., Doney, S. C., and Karl, D. M. (2011). Will ocean acidification affect marine microbes? *ISME J.* 5, 1–7. doi: 10.1038/ismej.2010.79

Kim, J.-M., Lee, K., Shin, K., Kang, J.-H., Lee, H.-W., Kim, M., et al. (2006). The effect of seawater CO_2 concentration on growth of a natural phytoplankton assemblage in a controlled mesocosm experiment. *Limnol. Oceanogr.* 51, 1629–1636. doi: 10.4319/lo.2006.51.4.1629

Kling, J. D., Lee, M. D., Fu, F.-X., Phan, M. D., Wang, X., Qu, P. P., et al. (2020). Transient exposure to novel high temperatures reshapes coastal phytoplankton communities. *ISME J.* 14, 413–424. doi: 10.1038/s41396-019-0525-6

Krumhardt, K. M. L., Lovenduskib, N. S., Iglesias-Rodriguezc, M. D., and Kleypasd, J. A. (2017). Coccolithophore growth and calcification in a changing ocean. *Prog. Oceanogr.* 159, 276–295. doi: 10.1016/j.pocean.2017.10.007

Le Quéré, C., Andrew, R., Canadell, J. G., Sitch, S., Korsbakken, J. I., Peters, G. P., et al. (2016). Global carbon budget 2016. *Earth Syst. Sci. Data* 8, 605–649.

Lee, K. H., Jeong, H. J., Lee, K., Franks, P. J., Seong, K. A., Lee, S. Y., et al. (2019). Effects of warming and eutrophication on coastal phytoplankton production. *Harm. Algae* 81, 106–118. doi: 10.1016/j.hal.2018.11.017

Li, F., Wu, Y., Hutchins, D. A., Fu, F., and Gao, K. (2016). Physiological responses of coastal and oceanic diatoms to diurnal fluctuations in seawater carbonate chemistry under two CO_2 concentrations. *Biogeosciences* 13, 6247–6259. doi: 10.5194/bg-13-6247-2016

Liao, Y., Feng, Y., Liu, Y., Li, W., Li, J., Ni, H., et al. (2019). The interative effects of nitrogen limitation and ocean acidification on the physiology of the coccolithophore *Emiliania huxleyi* NIWA 1108. *J. Tianjin Univ. Sci. Technol.* 34, 56–62. (In Chinese with English abstract),

Litchman, E., Klausmeier, C. A., Schofield, O. M., and Falkowski, P. G. (2007). The role of functional traits and trade-offs in structuring phytoplankton communities: scaling from cellular to ecosystem level. *Ecol. Lett.* 10, 1170–1181. doi: 10.1111/j.1461-0248.2007.01117.x

Martin-Jézéquel, V., Hildebrand, M., and Brzezinski, M. A. (2000). Review silicon metabolism in diatoms: implications for growth. *J. Phycol.* 36, 821–840. doi: 10.1046/j.1529-8817.2000.00019.x

McNair, H. M., Brzezinski, M. A., Till, C. P., and Krause, J. W. (2018). Taxon−specific contributions to silica production in natural diatom assemblages. *Limnol. Oceanogr.* 63, 1056–1075. doi: 10.1002/lno.10754

Mehrbach, C., Culberson, C. H., Hawley, J. E., and Pytkowic, R. M. (1973). Measurement of apparent dissociation cosntants of carbonic acid in seawater at atmospheric pressure. *Limnol. Oceanogr.* 18, 897–907. doi: 10.4319/lo.1973.18.6.0897

Milligan, A. J., Varela, D. E., Brzezinski, M. A., and Morel, F. M. (2004). Dynamics of silicon metabolism and silicon isotopic discrimination in a marine diatomas a function of pCO_2. *Limnol. Oceanogr.* 49, 322–329. doi: 10.4319/lo.2004.49.2.0322

Petrou, K., Baker, K. G., Nielsen, D. A., Hancock, A. M., Schulz, K. G., and Davidson, A. T. (2019). Acidification diminishes diatom silica production in the Southern Ocean. *Nat. Clim. Chang.* 9, 781–786. doi: 10.1038/s41558-019-0557-y

Raven, J. A., Cockell, C. S., and De La Rocha, C. L. (2008). The evolution of inorganic carbon concentrating mechanisms in photosynthesis. *Philos. Trans. R. Soc. Lond. B Biol. Sci.* 363, 2641–2650. doi: 10.1098/rstb.2008.0020

Raven, J. A., and Crawfurd, K. (2012). Environmental controls on coccolithophore calcification. *Mar. Ecol. Prog. Ser.* 470, 137–166. doi: 10.3354/meps09993

Riebesell, U., Wolfgladrow, D. A., and Smetacek, V. (1993). Carbon dioxide limitation of marine phytoplankton growth rates. *Nature* 361, 249–251. doi: 10.1038/361249a0

Riebesell, U., Zondervan, I., Rost, B., Tortell, P. D., Zeebe, R. E., and Morel, F. M. (2000). Reduced calcification of marine plankton in response to increased atmospheric CO_2. *Nature* 407, 364–367. doi: 10.1038/35030078

Rose, J. M., Feng, Y., Ditullio, G. R., Dunbar, R. B., Hare, C. E., Lee, P. A., et al. (2009). Synergistic effects of iron and temperature on Antarctic phytoplankton assemblages. *Biogeosciences* 6, 3131–3147. doi: 10.5194/bg-6-3131-2009

Rost, B., Riebesell, U., Burkhardt, S., and Sultemeyer, D. (2003). Carbon acquisition of bloom-forming marine phytoplankton. *Limnol. Oceanogr.* 48, 55–67. doi: 10.4319/lo.2003.48.1.0055

Schulz, K. G., Bach, L. T., Bellerby, R. G. J., Bermúdez, R., Büdenbender, J., Boxhammer, T., et al. (2017). Phytoplankton blooms at increasing levels of atmospheric carbon dioxide: experimental evidence for negative effects on prymnesiophytes and positive on small picoeukaryotes. *Front. Mar. Sci.* 4:64. doi: 10.3389/fmars.2017.00064

Sett, S., Schulz, K. G., Bach, L. T., and Riebesell, U. (2018). Shift towards larger diatoms in a natural phytoplankton assemblage under combined high-CO_2 and warming conditions. *J. Plankton Res.* 40, 391–406. doi: 10.1093/plankt/fby018

Sheridan, J. A., and Bickford, D. (2011). Shrinking body size as an ecological response to climate change. *Nat. Clim. Change* 1, 401–406. doi: 10.1038/nclimate1259

Smayda, T. J., and Boleyn, B. J. (1966). Experimental observations on the floatation of marine diatoms. II. *Skeletonema costatum* and *Rhizosolenia setigera*. *Limnol. Oceanogr.* 11, 18–34. doi: 10.4319/lo.1966.11.1.0018

Smayda, T. J., and Reynolds, C. S. (2003). Strategies of marine dinoflagellate survival and some rules of assembly. *J. Sea Res.* 49, 95–106. doi: 10.1016/s1385-1101(02)00219-8

Solórzano, L., and Sharp, J. H. (1980). Determination of total dissolved phosphorus and particulate phosphorus in natural waters. *Limnol. Oceanogr.* 25, 756–760.

Sommer, U., Adrian, R., Bauer, B., and Winder, M. (2012). The response of temperate aquatic ecosystems to global warming: novel insights from a multidisciplinary project. *Mar. Biol.* 159, 2367–2377. doi: 10.1007/s00227-012-2085-4

Sommer, U., Paul, C., and Moustaka-Gouni, M. (2015). Warming and ocean acidification effects on phytoplankton—from species shifts to size shifts within species in a mesocosm experiment. *PLoS One* 10:e0125239. doi: 10.1371/journal.pone.0125239

Spilling, K., and Lindström, M. (2008). Phytoplankton life cycle transformations lead to species-speci?c effects on sediment processes in the Baltic Sea. *Cont. Shelf Res.* 28, 2488–2495. doi: 10.1016/j.csr.2008.07.004

Spilling, K., Olli, K., Lehtoranta, J., Kremp, A., Tedesco, L., Tamelander, T., et al. (2018). Shifting diatom—dinoflagellate dominance during spring bloom in the Baltic Sea and its potential effects on biogeochemical cycling. *Front. Mar. Sci.* 5:327. doi: 10.3389/fmars.2018.00327

Taucher, J., Boxhammer, T., Bach, L. T., Paul, A. J., Schartau, M., Stange, P., et al. (2020). Changing carbon-to-nitrogen ratios of organic-matter export under ocean acidification. *Nat. Clim. Change* 11, 52–57. doi: 10.1038/s41558-020-00915-5

Thomas, C. R. (Ed.) (1997). *Identifying Marine Phytoplankton*. Amsterdam: Elsiever.

Tortell, P. D., Payne, C. D., Li, Y. Y., Trimborn, S., Rost, B., Smith, W. O., et al. (2008). CO_2 sensitivity of Southern ocean phytoplankton. *Geophys. Res. Lett.* 35, 1–5.

Tréguer, P., Bowler, C., Moriceau, B., Dutkiewicz, S., Gehlen, M., Aumont, O., et al. (2018). Influence of diatom diversity on the ocean biological carbon pump. *Nat. Geosci.* 11, 27–37. doi: 10.1038/s41561-017-0028-x

Utermöhl, H. (1958). Zur Vervollkommnung der quantitativen Phytoplankton-Methodik. *Mitt. Int. Ver. Theor. Angew. Limnol.* 9, 1–38. doi: 10.1080/05384680.1958.11904091

Varela, R., Lima, F. P., Seabra, R., Meneghesso, C., and Gómez-Gesteira, M. (2018). Coastal warming and wind-driven upwelling: a global analysis. *Sci. Total Environ.* 639, 1501–1511. doi: 10.1016/j.scitotenv.2018.05.273

Vehmaa, A., Kremp, A., Tamminen, T., Hogfors, H., Spilling, K., and Engström-Öst, J. (2011). Copepod reproductive success in spring-bloom communities with modified diatom and dinoflagellate dominance. *ICES J. Mar. Sci.* 69, 351–357. doi: 10.1093/icesjms/fsr138

Wasmund, N., Kownacka, J., Göbel, J., Jaanus, A., Johansen, M., Jurgensone, I., et al. (2017). The diatom/dinoflagellate index as an indicator of ecosystem changes in the Baltic Sea. 1. Principle and handling instruction. *Front. Mar. Sci.* 4:22. doi: 10.3389/fmars.2017.00022

Wu, R., Li, C., and Lin, J. (2017). Enhanced winter warming in the Eastern China Coastal Waters and its relationship with ENSO. *Atmos. Sci. Lett.* 18, 11–18. doi: 10.1002/asl.718

Wu, Y., Campbell, D. A., Irwin, A. J., Suggett, D. J., and Finkel, Z. V. (2014). Ocean acidification enhances the growth rate of larger diatoms. *Limnol. Oceanogr.* 59, 1027–1034. doi: 10.4319/lo.2014.59.3.1027

Xiao, W., Liu, X., Irwin, A. J., Laws, E. A., Wang, L., Chen, B., et al. (2018). Warming and eutrophication combine to restructure diatoms and dinoflagellates. *Water Res.* 128, 206–216. doi: 10.1016/j.watres.2017.10.051

Zhai, W., Zhao, H., Zheng, N., and Xu, Y. (2012). Coastal acidification in summer bottom oxygen-depleted waters in northwestern-northern Bohai Sea from june to august in 2011. *Chin. Sci. Bull.* 57, 1062–1068. doi: 10.1007/s11434-011-4949-2

Zhang, Y., Wang, T., Li, H., Bao, N., Hall-Spencer, J. M., and Gao, K. (2018). Rising levels of temperature and CO_2 antagonistically affect phytoplankton primary productivity in the South China Sea. *Mar. Environ. Res.* 141, 159–166. doi: 10.1016/j.marenvres.2018.08.011

Zou, L., Zhang, J., Pan, W. X., and Zhan, Y. P. (2001). *In situ* nutrient enrichment experiment in the Bohai and Yellow Sea. *J. Plankton Res.* 23, 1111–1119. doi: 10.1093/plankt/23.10.1111

Conflict of Interest: The authors declare that the research was conducted in the absence of any commercial or financial relationships that could be construed as a potential conflict of interest.